Design and optimization of an airflow-vibration sieving device for the effective cleaning of *cyperus esculentus* L. harvesting mixture

Shan Chen[1,2], Shiguan An[1,2], Za Kan[1,2], Lidong Huang[3], Hewei Meng[1,2], Jiangtao Qi[1,2*], Huijie Peng[1,2]

(1. *College of Mechanical and Electrical Engineering, Shihezi University, Shihezi 832000, Xinjiang, China*;
2. *Engineering Research Center for Production Mechanization of Oasis Special Economic Crop, Ministry of Education, Shihezi 832000, Xinjiang, China*;
3. *Guilin Mike Machinery Co., Ltd, Guilin 541000, Guangxi, China*)

Abstract: The threshing mixture of *Cyperus esculentus* (Tiger nut) planted in sandy areas is complex during harvesting, and there are problems of high impurity rate and high cleaning loss rate of the seeds. In this paper, the threshing mixture of *Cyperus esculentus* is taken as the research object, and the suspension speed of each component is measured to design an "airflow + vibration" sieving device. Use the vector polygon method to explore the law of motion of the vibrating sieve, establish the force model of the seeds on the sieve surface, and analyze the conditions for the seeds to penetrate the sieve. According to the principle of seeds penetrating the sieve and long stalks not penetrating the sieve, the geometric model of sieve blades opening degree adjustment mechanism is constructed. Study of the conditions under which long stalks can be thrown out of the machine. The experiment bench of the cleaning device was built, and the evaluation indexes were the rate of seed impurity and the rate of cleaning loss of the device, and the crank speed, sieve blades opening degree and fan speed were used as the experiment factors to study the influence law of each influencing factor on the evaluation index through single-factor experiment. Using response surface methodology to find the optimal combination of working parameters of the cleaning device. To verify the device's application on the combine harvester to improve the effectiveness of the cleaning operation of the *Cyperus esculentus* combine harvester.

Keywords: sand cultivation, *Cyperus esculentus*, wind sieve type cleaning device, optimization
DOI: 10.25165/j.ijabe.20241704.8359

Citation: Chen S, An S G, Kan Z, Huang L D, Meng H W, Qi J T, et al. Design and optimization of an airflow-vibration sieving device for the effective cleaning of *cyperus esculentus* L. harvesting mixture. Int J Agric & Biol Eng, 2024; 17(4): 77–88.

1 Introduction

China's dependence on soybean imports continues to grow - with implications reaching 100.327 Mt in 2020, accounting for 94.5% of total domestic edible oilseed imports[1-3]. It has become essential to find alternative oilseed crops. *Cyperus esculentus*, as a new type of oilseed crop, not only has the potential to reduce the demand for soybean imports but also plays a vital role in ecological restoration and soil improvement in the southern Xinjiang Uygur Autonomous Region (XUAR) due to its well-developed root system and lush stems and leaves[4-6]. Although *Cyperus esculentus* is widely cultivated in over 20 provinces, including Xinjiang, Jilin, Inner Mongolia, and Guangdong[7], its harvesting process still faces significant challenges. Especially in the sandy areas of southern Xinjiang, the harvesting of *Cyperus esculentus* is even more difficult due to the special cultivation environment, which has become a key factor restricting the development of the industry.

International research on *Cyperus esculentus* has focused on food health and seed characterization[8,9], while most domestic mechanized harvesting technologies have been achieved through improved harvesting equipment for other crops[10]. The clearing is a critical link in mechanized harvesting. Its performance directly affects the overall operational efficiency. In the mechanized harvesting of *Cyperus esculentus* in the sandy areas of the southern border, a rotary tiller is used to propel the material, and a conveyor mechanism is used to lift the material. Then, it is passed through a double-decker screen cage for threshing and separation and a vibrating screen to remove secondary impurities. However, the existing machines, as a whole, face challenges such as high failure rates, excessive energy consumption, high bean losses, and high impurity levels[10]. In response to these problems, this study develops adapted devices starting from the *Cyperus esculentus* scavenging process.

Harvester cleaning devices are categorized into single airflow type, single vibrating screen type, and combined air-screen type[11-14]. These technologies excel at cleaning conventional crops such as wheat, peanuts, corn, and canola but are not as effective at cleaning specialty crops such as *Cyperus esculentus*. For example, Dai et al.[15], Yang et al.[16], and Wang et al.[17] have conducted in-depth studies on the scavenging problems of flaxseed, peanut film seed,

Received date: 2023-03-17 **Accepted date:** 2024-04-08
Biographies: Shan Chen, PhD candidate, research interest: agricultural robotics, Email: chenshan1@stu.shzu.edu.cn; **Shiguan An**, MS, research interest: agricultural machinery, Email: 384055210@qq.com; **Za Kan**, Professor, research interest: agricultural machinery, Email: kz-shz@163.com; **Lidong Huang**, Senior Engineer, research interest: agricultural machinery, Email: zhuojie1@163.com; **Hewei Meng**, Professor, research interest: agricultural machinery, Email: mengbai4251982@sina.com.; **Huijie Peng**, MS, research interest: agricultural machinery, Email: Gump777@88.com.
***Corresponding author: Jiangtao Qi**, Associate Professor, research interest: agricultural machinery. College of Mechanical and Electrical Engineering, Shihezi University, Shihezi 832000, Xinjiang, China. Tel: +86-15699322648, Email: 510014078@qq.com

and corn, respectively. Meanwhile, the research of Li et al.[18] and Xu et al.[19] focused on the adaptive monitoring and optimization of the scavenging device. In addition, Geng et al.[20] explored the effects of vibrating screen amplitude, frequency, fan speed, inclination angle, and other factors on scavenging efficiency. Based on these studies, Liu et al.[21] developed a multifunctional harvester, which improved clearing efficiency by integrating modular vibratory screening and airflow separation technologies. However, none of the above studies involved the analysis of the motion trajectories of the components of the mixtures; Qu et al.[22] did not explore the effect of sieve size on the screening effectiveness of different sizes of *Cyperus esculentus*, although they used fixed woven sieve apertures to separate *Cyperus esculentus* from straw and soil. Similarly, He et al.[23] did not consider the motion characteristics of the components under external excitation, although they developed a lifting sieve with adjustable mesh.

This study aimed to develop an efficient, reliable, and structurally simple cleaning device for the sandy cultivation of *Cyperus esculentus*. The goals of this research include (1) improving the screening and sorting capacity of the cleaning mechanism and optimizing the airflow and vibration parameters for more efficient cleaning; (2) improving the cleaning efficiency and quality by optimizing the operating parameters and the movement paths of the components; (3) designing an energy-efficient and environmentally friendly device to reduce the energy consumption and the impact on the environment; and (4) ensuring, through experimental validation and performance evaluation, the designed device's efficiency and reliability of the designed device. This paper demonstrates the potential and advantages of this cleaning device in the mechanized harvesting of *Cyperus esculentus* through system analysis and experimental validation.

2 Device design

2.1 Device structure

Wind sieve type *Cyperus esculentus* cleaning device, mainly by the frame, cross-flow fan, connecting rod and rocker mechanism, sieve surface inclination adjustment mechanism, sieve blade opening degree adjustment mechanism, vibrating sieve, eccentric wheel, top cover, diversion hood, and other components, forms the overall structure of the device as shown in Figure 1.

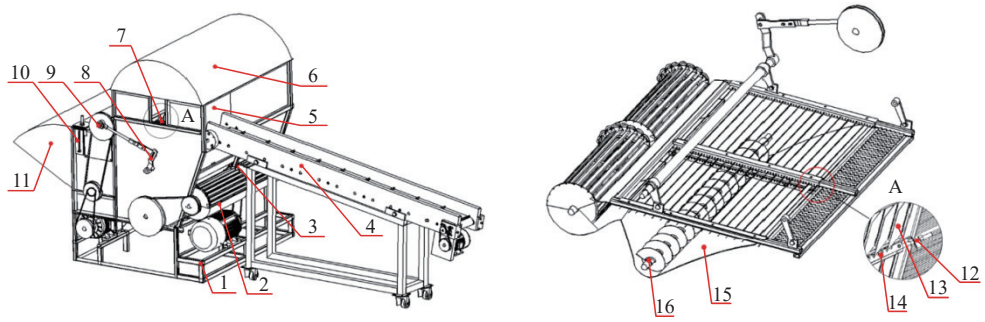

a. Wind sieve type cleaning device b. Vibrating sieving mechanism

1. Frame 2. Cross-flow fan 3. Fixed mechanism 4. Conveyer 5. Feed opening 6. Top cover 7. Vibrating sieve 8. Connecting rod and rocker mechanism 9. Eccentric wheel 10. sieve blades opening degree adjustment mechanism 11. Diversion hood 12. Adjustment mechanism of sieve blades opening degree 13. Shutter sieve blade 14. Middle beam 15. Slide 16. Collecting churn

Figure 1 Wind sieve type cleaning device for *Cyperus esculentus* structural diagram

Device working principle: A certain amount of oleaginous bean stripping mixture is evenly spread on the conveyor belt. Before the experiment, adjust the inverter controlling the conveyor, vibrating screen, and fan to the required frequency. At the beginning of the experiment, first turn on the frequency converter controlling the vibrating sieve and the fan, and then start the conveyor frequency converter when the motor speed reaches the specified speed. The mixture of threshing material (seeds, broken beans, stalks, shriveled beans, and lightweight miscellaneous residue) is conveyed by the conveyor to the feed opening for feeding. The motor controlling the vibrating sieve drives the eccentric wheel to rotate, driving the rocker and linkage mechanism to do plane movement, thus driving the vibrating screen to swing. The motor controlling the fan drives the fan spindle to rotate, thus generating airflow. The airflow from the outlet of the cross-flow fan penetrates the sieve from below and acts on the material, and the fan spindle makes the seeds collect and convey by the belt drive.

Due to the synergistic operation of the cross-flow fan and the vibrating sieve body, the fed offcuts are thrown several times by the vibrating screen. The cross-flow fan generates airflow to disperse the material being thrown up. Due to differences in physical properties in the detritus, differential motion will occur in each group. During this process, the seeds are sieved through the sieve and transported by the collecting churn to the discharge port for manual collection. And the impurities are discharged from the rear diversion hood of the cleaning device to complete the separation of seeds and miscellaneous residues.

2.2 Measurement of suspension speed of each component

The determination of the suspension speed of each component is the key to setting the airflow velocity inside the device. As in Figure 2, the suspension speed of the five components of the threshing mixture was measured using the WXS-1 agricultural material suspension experiment bench, including *Cyperus esculentus*, stalks, broken beans, shriveled beans, and light debris (grass and fibrous root aggregates). Since the size distribution of each component in the threshing mixture of *Cyperus esculentus* varies greatly, direct measurement can cause large errors. Randomly select 100 beans using the five-point sampling method[24]. The high triaxial dimension was chosen as the classification criterion to classify them into three particle-size classes. Height: less than 8 mm for small-sized beans and more than 8 mm for big-sized beans. Similarly, the length of the stalk was taken as the classification criterion, less than 30 mm as short stalks, and more than 30 mm as long stalks.

According to the "Forage Seed Suspension Speed Determination Method", 25 g of each of the two-grain sizes of

Cyperus esculentus, two lengths of stalks, broken beans, shriveled beans, and lightweight miscellaneous residue were weighed with an electronic scale. As in Figure 3, the suspension speed was measured separately for each component.

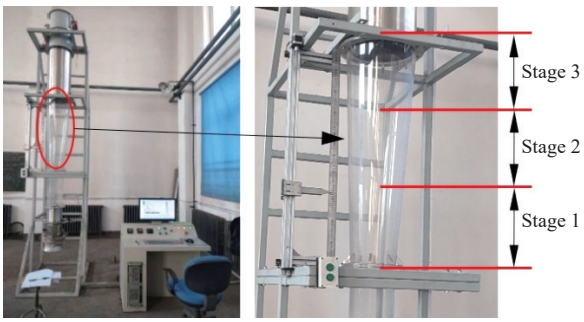

Figure 2 WXS-1 agricultural material suspension experiment bench

a. Seed b. Broken bean

c. Stalk d. Shriveled bean

e. Lightweight miscellaneous residue

Figure 3 Components of the threshing mixture

The maximum wind speed at the exit of the cross-flow fan on the experiment bench should not be higher than the suspension speed of small-sized beans. The conical tube of the suspension experiment bench is the material suspension speed measurement area, divided evenly into three zones according to height. Press the start button to set the suspension speed of the material just entering stage 1 as the minimum and the suspension speed of the material just entering stage 3 as the maximum.

The suspension speed is calculated as shown in Equation (1).

$$H = v\left(\frac{190}{190+2h\tan\alpha}\right) \tag{1}$$

where, H is suspension speed, m/s; v is air speed, m/s; h is suspension height, mm; α is fan installation angle, (°); The value of the α is 3.5°.

Figure 4 shows the distribution of the overall suspension speed range of short stem, long stem, broken bean, small-sized bean, big-sized bean, and shriveled bean in the threshing mixture.

The lightweight miscellaneous residue suspension speed value is too low for the suspension experiment bench sensor to detect. Therefore, the use of airflow can remove all lightweight miscellaneous residues from the machine. The big-sized bean third-stage suspension speed value is too high and exceeds the fan air speed range; the mean suspension speed of the two was significantly different from that of other components. The maximum and minimum suspension speeds of short stems are lower than those of the other components, and a single airflow can separate them. However, there was overlap in the suspension speeds of shriveled beans, short stems, long stems, broken beans, small-sized beans, and big-sized beans. Single air flow separation does not provide a good separation of broken beans, small-sized beans, and big-sized beans from the threshing mixture. Therefore, in order to separate and clean *Cyperus esculentus*, the "airflow + vibration" method is used for cleaning operations.

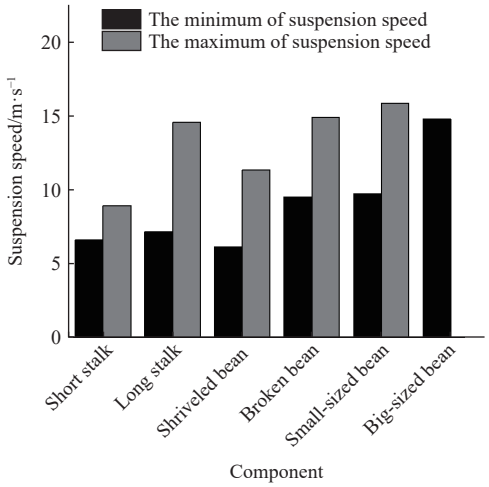

Figure 4 Distribution of overall suspension speed intervals in three stages

2.3 Study of the cleaning process

When the “airflow + vibration” method is used for cleaning operations. Theoretically, a single airflow can blow all the lightweight miscellaneous residue and short stems, some long stems, and most of the shriveled beans out of the machine, but considering that the material fed has a certain thickness, there may be a small amount of doping in it. The doped part and the remaining part require the vibration of the sieve body to work synergistically with the fan air flow to separate the *Cyperus esculentus* from the threshing mixture.

2.3.1 Vibrating sieve motion law

As shown in Figure 5a, the upper end of the front pendulum of the vibrating sieve is fixed to the frame; eccentric wheel eccentricity can be considered a crank; eccentric wheel rotation drives the movement of the connecting rod and rocker, which drives the reciprocating motion of the vibrating sieve. The motion analysis of the vibrating sieve motion process is carried out by the closed vector polygon method[25] of the analytical method. Establishing a rectangular coordinate system, the sketch of the mechanism’s movement is shown in Figure 5b, each rod in the mechanism can be represented as a corresponding rod vector, and each rod vector forms a closed vector polygon.

$$\underset{l_1}{\rightarrow} + \underset{l_2}{\rightarrow} - \underset{l_3}{\rightarrow} - \underset{l_4}{\rightarrow} = 0 \tag{2}$$

Projecting Equation (2) onto the x-axis and y-axis, respectively, Equation (3) can be obtained:

$$\begin{cases} l_1\cos\theta_1 + l_2\cos\theta_2 = l_3\cos\theta_3 + l_4 \\ l_1\sin\theta_1 + l_2\sin\theta_2 = l_3\sin\theta_3 \end{cases} \tag{3}$$

Deriving Equation (3) for time t, the following equation can be obtained:

$$\begin{cases} l_1\omega_1\cos\theta_1 + l_2\omega_2\cos\theta_2 = l_3\omega_3\cos\theta_3 \\ l_1\omega_1\sin\theta_1 + l_2\omega_2\sin\theta_2 = l_3\omega_3\sin\theta_3 \end{cases} \tag{4}$$

Combining Equation (4) with the derivative for time t and re-organizing it, then Equation (5) can be obtained:

$$\begin{cases} \alpha_3 = \dfrac{\omega_1^2 l_1\cos(\theta_1-\theta_2) + \omega_2^2 l_2 - \omega_3^2 l_3\cos(\theta_3-\theta_2)}{l_3\sin(\theta_3-\theta_2)} \\ \alpha_2 = \dfrac{-\omega_1^2 l_1\cos(\theta_1-\theta_3) + \omega_2^2 l_2\cos(\theta_2-\theta_3) - \omega_3^2 l_3}{l_2\sin(\theta_2-\theta_3)} \end{cases} \tag{5}$$

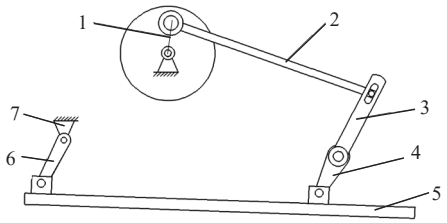

a

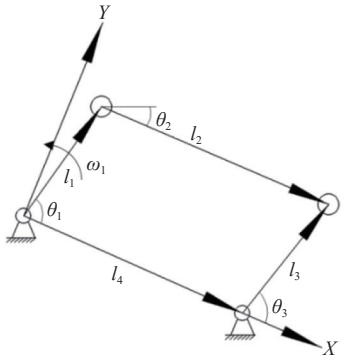

b

Figure 5 Vibrating sieve drive mechanism model and mechanism movement sketch

Integrating the acceleration yields the rocker velocity equation. The rocker trajectory equation is obtained by double integration of the acceleration.

From the above, it is clear that the trajectory of the rocker at any point during its motion is simple harmonic motion with a fixed amplitude; acceleration is the image of the sine and cosine functions; similarly, the velocity and displacement follow a similar trend.

2.3.2 Seed motion law

Figure 6 shows the force analysis of the movement of the seeds on the vibrating sieve under the action of "airflow+vibration". Acceleration $a > 0$, a vibrating sieve accelerates upward motion or accelerates downward motion; correspondingly, the seeds slide downwards or upwards. When the vibrating sieve decelerates upward or downward, the acceleration is 0, and the seeds slide upward or downward. According to the suspension speed in 2.1, the beans were all suspended at a greater rate than the other threshing mixture, and as expected, the beans fell through the sieve surface to the winch below. Therefore, only the beans sliding down the sieve face are analyzed, as shown in Figure 6.

The equation for the mechanics of the seeds on the sieve surface is shown below. When the sieve surface accelerates upward or decelerates downward, the equilibrium equation for the forces on the particles on the sieve is established and analyzed.

$$\begin{cases} T = G\cos\alpha \pm u\sin(\gamma-\alpha) - F\sin(\beta-\alpha) \\ F = G\sin\alpha \pm u\cos(\gamma-\alpha) - f - F\cos(\beta-\alpha) \end{cases} \tag{6}$$

$$G = mg \tag{7}$$

Among them

$$f = T\tan\delta \tag{8}$$

$$u = m\omega_3^2 r\sin(\omega_3 t) \tag{9}$$

$$F = \frac{Sv^2}{1600}\times 10^3 \tag{10}$$

Substituting into the above equations, the following equation can be obtained:

$$\begin{cases} T = mg\cos\alpha \pm m\omega_3^2 r\sin(\omega_3 t)\sin(\gamma-\alpha) - \dfrac{Sv^2}{1600}\times 10^3\sin(\beta-\alpha) \\ F = mg\sin\alpha \pm m\omega_3^2 r\sin(\omega_3 t)\cos(\gamma-\alpha) - T\tan\delta - \\ \qquad \dfrac{Sv^2}{1600}\times 10^3\cos(\beta-\alpha) \end{cases} \tag{11}$$

where, T is the support force of the seeds on the sieve, N; G is the bean's own gravity, N; F is the air flow suspension force on the seeds, N; f is the sliding friction of the seeds on the sieve surface, N; u is the inertial force on the seeds, N; α is the installation angle of vibrating sieve, (°); β is the airflow direction angle, (°); γ is the vibration direction angle of sieve surface, (°); δ is the friction angle between grain and sieve surface, (°); ω_3 is the angular velocity of the rocker in 2.3.1, rad/s; S is the average windward area of the seeds, mm^2; v is the surface wind speed of seeds, m/s.

If $T > 0$, the seeds slide down the sieve face; on the contrary, they are thrown up by the sieving surface. When $F>0$, the particles slide backwards along the sieve; when $F<0$, the seeds are stationary. According to the analysis of Equation (11), when the acceleration of

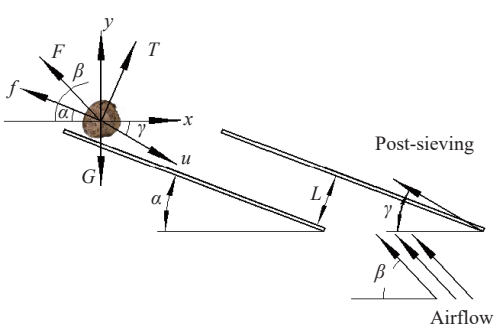

a. The vibrating sieve accelerates upward and the seeds slide downward

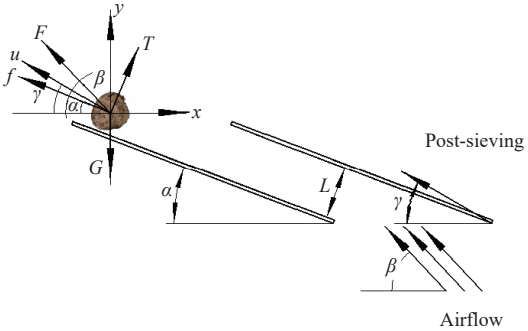

b. The vibrating sieve decelerates downward and the seeds slide downward

Figure 6 Schematic diagram of the forces on the seeds in different states of motion on the sieve surface

the sieve surface is positive, the sieve surface accelerates upward. To ensure that the seeds slide downward, the crank speed can be increased appropriately and the airflow speed can be reduced appropriately. When the acceleration of the sieve surface is negative, the sieve surface decelerates and moves downward. To ensure that the seeds slide downward, the crank speed should not be too high; too high tends to make the beans slide backward and throw them out, resulting in the loss of seeds. The crank speed experiment range is selected from 200 to 600 r/min. The airflow speed should not be too high; the maximum air speed at the outlet of the cross-flow fan of the experiment bench should not be higher than the minimum value of the suspension speed of small-sized beans. Select the fan speed experiment range of 600-1000 r/min.

2.3.3 The process of sieve blades opening degree adjustment

Figure 7a shows the sieve blade opening degree adjustment mechanism, which is located at the bottom of the sieve surface. Short columns are welded on the top and bottom of the sieve blade. In the middle beam and the lower lever on both sides, there are evenly distributed round holes. When the sieve blades are installed, the short columns on the left and right sides of the upper end of the sieve blades are inserted into the round holes on the left and right sides of the middle beam, and the short columns on the left and right sides of the lower end of the sieve blades are inserted into the round holes on the left and right sides of the lower lever. The round holes are all slightly larger in diameter than the short column, so that the short column can rotate freely in the round holes. The fixed block is located in the center of the rear end of the left and right lower levers and is welded to the sieve body. The left and right sides of the lower tie bar are fixed on both sides of the movable block by bolting, here, the lower lever and the movable block as a whole are fixed in the fixed block by means of a long screw post, which is secured by a locking nut.

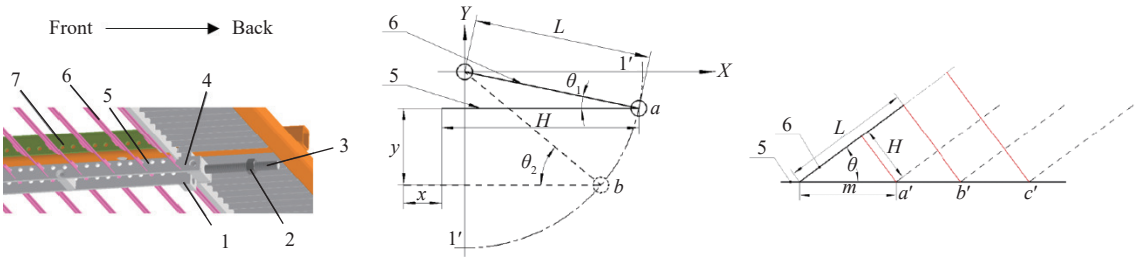

a.Sieve blades opening degree adjustment mechanism b. Sieve blades opening degree adjustment c. Sieve opening degree determination

1. Fixed block 2. Lock nut 3. Spiral column 4. Movable block 5. Lower lever 6. Sieve blade 7. Middle beam

Figure 7 Vibrating screen blade opening adjustment process

The sieve blade opening degree adjustment process is as follows: rotate the spiral column anticlockwise to drive the lower lever forward; at this time, the sieve blades rotate and the lower lever is positioned forward relative to the middle beam. The sieve blades rotate at different angles, and the opening degrees of two adjacent sieve blades are different. Use a vernier caliper to measure the sieve blades opening degree, stop the spiral column rotation after adjusting the sieve blades opening degree to meet the demand, and lock it with the lock nut to prevent the spiral column from loosening during the vibration of the vibrating sieve.

Figure 7b shows the principle of sieve blade opening degree adjustment; the trajectory of the lower tie rod is a quarter arc of 1′-1′. The process of adjusting the sieve opening is similar to the process of crank slider movement. In the figure, the sieve opening gradually increases during the change of position of the lower lever from *a* to *b*. In order to ensure that the impurities are thrown out of the machine backward, the sieve should be tilted backward, i.e., the lower lever movement track is in the fourth quadrant.

The sieve blades opening degree increased when the sieve blades rotated from position *a* to position *b*. The length of the spiral column to be adjusted is *x*, and the distance between the two centers of the fixed block U-shaped groove is *y*.

$$\begin{cases} x = L(\cos\theta_1 - \cos\theta_2) \\ y = L(\sin\theta_2 - \sin\theta_1) \end{cases} \tag{12}$$

where, L is the distance between the upper end of the sieve and the middle beam round hole connection to the lower end of the sieve and the lower lever round hole connection, mm; θ_1 is the angle between the sieve blades and the lower lever when the spiral column is in the upper limit position of the movable block (°), which is the minimum value of the sieve opening degree; θ_2 is the angle between the sieve blades and the lower lever when the spiral column is in the lower limit position of the movable block (°), which is the maximum value of the sieve opening degree.

In Figure 7c, a',b',c' are the three installation positions of adjacent sieve blades, and when the adjacent sieve blades are at a'.

$$H = m\sin\theta \tag{13}$$

where, H is the opening degree of two adjacent sieve blades, mm; m is the distance between the short cylinder on one side of the lower end of the two adjacent sieves and the connection of the round hole of the lower lever on one side, mm; θ is the rotation angle of the sieve blade, (°).

When the adjacent sieves are at b'

$$H = L\tan\theta \tag{14}$$

As can be seen from the figure, b' is the critical position of a', and the installation position of adjacent sieve blades cannot exceed b'; when it is in c', the sieve blades opening degree measurement needs to be on the extension line of the previous sieve, which does not meet the requirements.

In order to meet all the beans can penetrate the sieve, according to the size of big-sized bean to determine the minimum opening degree of the sieve for 15 mm; To ensure that the long stalks do not penetrate the sieve, the maximum opening of the sieve is 35 mm. When setting L to 45 mm, it is calculated that θ_1 is 18.43°, θ_2 is 37.87°, the center distance (m) between two adjacent circular holes at the bottom of two adjacent sieves connected to the lower lever is 50 mm, the length (x) of the spiral column to be adjusted is 7.17 mm, and the center distance (y) between the two centers of the fixed block U-slot is 13.40 mm.

2.3.4 Long stalk movement pattern

When long stalks are thrown upwards, the *Cyperus esculentus*

in the stalk layer has a larger mass and greater inertia. *Cyperus esculentus* and other components (shriveled beans, long stalks) are displaced to varying degrees in the upthrown stalk layer. The conditions that ensure that the seeds can fall have been analyzed in 2.3.2. To ensure that the long stalks can be discharged smoothly from the machine, a long leap is required, which depends on the height of the stalk layer thrown upwards and the height of the free fall. In order to make the free fall as high as possible, the sieve surface should collide with the stalk layer at the lowest possible position. To simplify the model, masses are used instead of stalks, and it is assumed that the masses do not slide on the inclined sieve surface. The trajectory of the long stalk movement is shown in Figure 8.

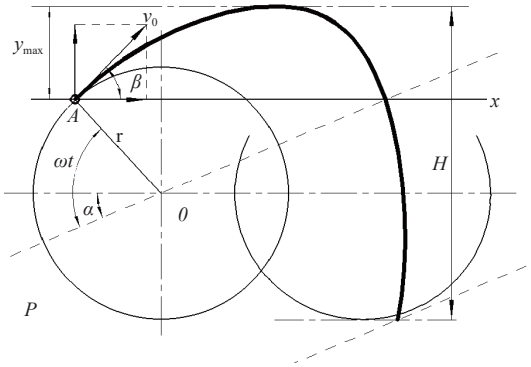

Figure 8 Stalk movement process

Let X be the tilt direction of the sieve surface, and OP is the horizontal surface. If the mass is located at the sieve surface A for the critical throwing position, the initial time is t. In the initial velocity V_0 under the action of the first upward throwing motion, after reaching the highest point to do free fall motion, the last drop to contact the sieve surface time is t'. From the figure, the height H of the free fall of the mass is:

$$H = y_{\max} + r\sin(\omega t - \alpha) + r \tag{15}$$

where, α is the angle between the sieve surface and the horizontal surface, (°); ωt is the angle of rotation of the crank with respect to the horizontal plane, (°); r is the crank length, mm.

where the critical condition for the mass to be thrown off the sieve surface is:

$$\sin\omega t \geq \frac{g\cos\alpha}{\omega^2 r} \tag{16}$$

The vertical distance between the highest point of the mass thrown off the sieve surface and the initial sieve surface is:

$$y_{\max} = \frac{(v_0\sin^2\beta)}{2g} \tag{17}$$

Among them

$$\beta = \frac{\pi}{2} + \alpha - \omega t \tag{18}$$

$$v_0 = \omega r \tag{19}$$

It is known that the time for one revolution of the crank is

$$T = \frac{2\pi}{\omega} \tag{20}$$

where, v' is the average speed of stalk movement, m/s.

$$v' = \frac{\sqrt{\omega^2 r}}{2\pi\cos\alpha}[\sin(\omega t' - \alpha)(t' - t) - \cos(\omega t - \alpha) + \cos(t' - \alpha)] \tag{21}$$

Among them

$$\omega t' = 2\pi - \omega t \tag{22}$$

The horizontal distance of the stalk leaping over the sieve surface is

$$L = v'T \tag{23}$$

According to the literature[26], the peanut pod cleaning device vibrating sieve vibrates at a frequency of 5.5 Hz for high operational efficiency. *Cyperus esculentus* are similar to peanut seeds, and the minimum value of crank speed n is selected as 200 r/min (f= 3.33 s^{-1}). When the crank length is r is 0.035 m, the sieve inclination angle α is 8°, the calculation can be obtained from the highest point of the mass thrown off the sieve surface and the initial vertical distance of the sieve surface y_{max} is 0.35 m, H is 0.4 m. and the total length of the sieve surface L is 1 m. To ensure that the long stalks are successfully thrown out of the machine, the end of the sieve surface is set up as a keyed sieve.

3 Materials and methods

3.1 Experiment materials

The experiment was conducted in the 54th regiment of the 3rd division of the Xinjiang Production and Construction Corps. The experiment's *Cyperus esculentus* variety was Chinese *Cyperus esculentus* No.1. Figure 9 shows the *Cyperus esculentus* beans to be harvested by the 54th Regiment of the 3rd Division. The sample material was obtained from Lot 39. According to the depth of *Cyperus esculentus* planting, the *Cyperus esculentus* plants with soil at a depth of 12 cm below ground were excavated manually, and the soil wrapped by the root system was gently shaken off, collected, and transported to the experiment site as feed material for the threshing machine.

Figure 9 *Cyperus esculentus* planting area of 54 regiments in South Xinjiang region

The threshing device limits the feed rate to 3 kg/s. The feeding quantity of the cleaning device is less than the feeding quantity of the threshing device. Under normal conditions, when the threshing unit is fed with 2 kg/s, the collected threshing mixture under the concave plate sieve, weighing 1.3 kg/s, is used as the feeding volume of the cleaning device. The fed threshing mixture consisted of five main components: beans, shriveled beans, short stalks, long stalks, broken beans, and lightweight miscellaneous residue. (Since the beans are wrapped by intertwined hairy roots and have a high moisture content, they are easily broken during the threshing process and form broken beans; the fluffy dead leaves on the outside of the stubble are easily rubbed off during the threshing process, leaving a fine stalk with a clean surface; beans that were missed in the previous harvest and rotted in the ground to form shriveled beans; the remaining hairy bearded roots, broken roots, and shredded grass were lightweight miscellaneous residue). Of these, the percentage of bean mass was about 71.28%, the

percentage of broken bean mass was about 6.31%, the percentage of stalk mass was about 3.61%, the percentage of shriveled bean mass was about 0.90%, and the percentage of lightweight miscellaneous residue mass was about 17.9%. The above components were prepared in this mass ratio and used as feeding materials for each group of experiments.

Referring to the national standard "GB/T 14489.1-2008 Determination of Moisture and Volatile Matter Content of Oilseeds", using the 101-IB electric blast thermostatic drying oven, the moisture content of each component of the *Cyperus esculentus* threshing mixture was measured three times to take the average value, and the moisture content of the beans was measured to be 28.20%, the moisture content of stalks was 10.20%, the moisture content of shriveled beans was 15.74%, and the moisture content of lightweight miscellaneous residue was 14.05%. The performance experiment of the cleaning device was carried out at this moisture content combination.

3.2 Experiment methodology

Adjust the crank speed of the vibrating sieve by adjusting the frequency of the inverter controlling the eccentric wheel; regulate the spindle speed of the fan by adjusting the frequency of the inverter controlling the fan; and adjust the sieve blades opening degree by turning the long screw in the sieve blades opening degree adjustment mechanism. Idle operation check of the device before the experiment. Adjust the frequency converter so that the spindle speed of the conveyor belt reaches 200 r/min. Measurements are selected to divide the area of the conveyor belt corresponding to the feeding volume by 1 s. The prepared material is mixed evenly and laid flat on the bottom of the conveyor belt in the area of 1 s. Allow a certain displacement for the conveyor idling operation to return to normal working condition. Make sure the uniformly mixed materials are fed into the cleaning device at a uniform speed. Running the frequency converter of the vibrating sieve, fan and conveyor belt in sequence, take out the cleaning discharge at the side of the cleaning device—the discharge port of the collecting and transporting churn and under the rear diversion hood, respectively. Each group of experiments was repeated three times to take the average value as the experiment result.

3.3 Evaluation indicators

Referring to the national standard "seed cleaning machine experiment methods", the wind sieve type primary cleaning machine seed impurity rate is less than or equal to 6%. According to the actual production requirements, the scavenging loss rate should be as small as possible, set at less than or equal to 4%. The seed impurity rate and the cleaning loss rate were used as indicators to evaluate the operational performance of the wind sieve-type *Cyperus esculentus* cleaning device. The specific calculation is as follows:

Seed impurity rate:

$$Y_1 = \frac{\sum W_a}{\sum W_g} \times 100\% \tag{24}$$

where, W_a is the weight of impurities at the discharge port of the churn under the sieve, kg; W_g is the total weight of discharges at the discharge port of the churn under the sieve, kg.

Clearance loss rate:

$$Y_2 = \frac{\sum W_b}{\sum W_q} \times 100\% \tag{25}$$

where, W_b is the weight of the seeds under the diversion hood, kg; W_q is the total weight of the seeds fed into the feed opening, kg.

4 Results and discussion

4.1 Single-factor experiment

According to the device design, it is known that the device crank speed, fan speed, and sieve blade opening degree have a great influence on the cleaning performance. To improve the efficiency of cleaning operations, a single-factor experiment was conducted[24]. The other two factors need to be fixed for each group of single-factor experiments to study the effects of changing factors on the rate of seed impurity and cleaning loss rate. The experiment parameters are as follows: crank speed 200-600 r/min, fan speed 600-1000 r/min, sieve blade opening degree of 15-35 mm. The values of fixed factors for each group of single-factor experiments were: crank speed 400 r/min, fan speed 800 r/min, and sieve blade opening degree 25 mm, and each group of experiments was repeated three times. The variation pattern of the seed impurity rate and cleaning loss rate with each single factor are shown in Figure 10.

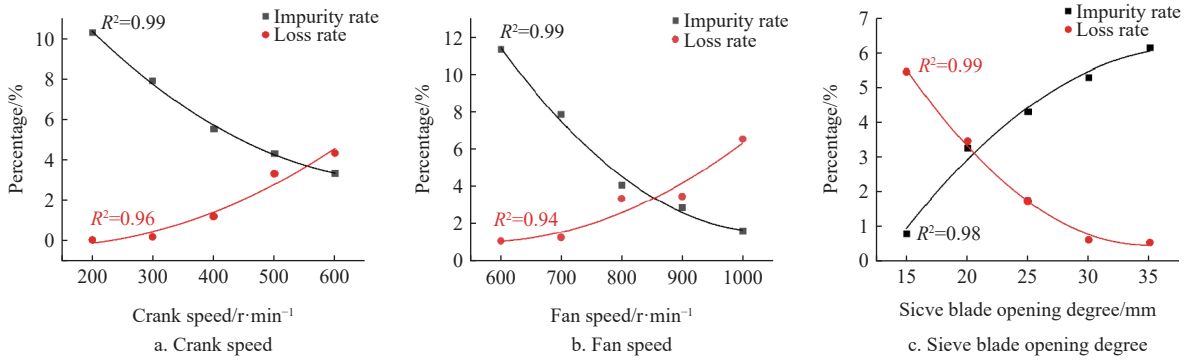

Figure 10 Variation of seed impurity rate and cleaning loss rate with each single factor

As can be seen from Figure 10a, with the increase in crank speed, the seed impurity rate of the threshing mixture of *Cyperus esculentus* gradually decreased and the cleaning loss rate gradually increased. With a crank speed of 300 r/min, seed impurity rate is more than 6%; when the crank speed is 600 r/min, the cleaning loss rate is greater than 4%; take the crank speed experiment range of 400-500 r/min. Figure 10b shows that as the fan speed increased, the impurity rate of the threshing mixture of *Cyperus esculentus* gradually declined and the loss rate gradually increased. The impurity rate was higher than 6% when the fan speed was 700 r/min, and the cleansing loss rate was higher than 4% when the fan speed was 1000 r/min. The fan speed range was between 800 and 900 r/min. Figure 10c shows that the loss rate progressively decreased while the impurity rate of the *Cyperus esculentus* seed

threshing mixture gradually rose with the increasing sieve blade opening degree. The loss rate was higher than 4% when the sieve blades' opening degree was 15 mm, and the seed impurity rate was higher than 6% when it was 35 mm. The measurement range for the sieve blades' opening degree was 20-30 mm.

4.2 Response surface experiments

4.2.1 Response surface methodology

Combining the aforementioned single-factor experimental analysis and results, a three-factor, three-level experimental design was carried out using the Box-Behnken experimental design method[27]. Crank speed (X_1), fan speed (X_2), and sieve opening degree (X_3) were used as independent variables, and seed impurity rate (Y_1) and cleaning loss rate (Y_2) were used as response values. Each experimental factor was coded as shown in Table 1, with 17 experiment points and 12 analytical variables in each. Table 2 displays the experiment procedure and outcomes.

Table 1 Coding value of experiment factors

Code	Factor		
	Crank speed X_1/(r·min^{-1})	Fan speed X_2/(r·min^{-1})	Sieve blade opening degree X_3/mm
–1	400	800	20
0	450	850	25
1	500	900	30

Table 2 Experimental scheme design and results

Crank speed	Fan speed	Sieve blade opening degree	Impurity rate/%	Loss rate/%
–1	–1	0	5.83	0.77
1	–1	0	1.16	2.04
–1	1	0	2.7	1.25
1	1	0	1.53	2.39
–1	0	–1	5.3	1.64
1	0	–1	2.27	2.65
–1	0	1	5.21	0.43
1	0	1	2.98	1.75
0	–1	–1	4.53	1.5
0	1	–1	3.52	2.1
0	–1	1	5.78	0.39
0	1	1	3.02	0.75
0	0	0	1.72	1.04
0	0	0	1.77	0.93
0	0	0	1.64	1.01
0	0	0	1.74	0.98
0	0	0	1.44	1.02

4.2.2 Regression modeling and significance testing

Regression model analysis was performed on the experimental data, and the regression equation was used to estimate the extreme value point and find the optimal pairing. Let the regression equation be[28].

$$Y = b_0 + \sum_{i=1}^{k} b_i X_i + \sum_{i=1}^{j=1} \sum_{j=1}^{k} b_{ij} X_i X_j + \sum_{i=1}^{k} b_{ii} X_{i^2} \quad (26)$$

where, Y is the response value, b_0 is the random error, b_i is the primary term coefficient, b_{ij} is the interaction term coefficient, b_{ii} is the quadratic term coefficient, X_i is the primary term variable, X_iX_j is the interaction term variable, and X_{i^2} is the quadratic term variable.

To establish the regression models of the impurity rate (Y_1) and loss rate (Y_2) on the three independent variables of crank speed (X_1), fan speed (X_2), and sieve blade opening degree (X_3), the regression model ANOVA on the experiment results in Table 2 was carried out using Design-Expert.8.0.6 software. The results are listed in Table 3.

Table 3 Variance analysis of regression model

Experimental indexes	Source	Sum of square	Degree of freedom	F-value	p-value	Significant
Y_1	Model	43.40	9	139.15	<0.0001	**
	X_1	15.40	1	444.47	<0.0001	**
	X_2	5.33	1	153.82	<0.0001	**
	X_3	0.23	1	6.77	0.0353	*
	X_1X_2	3.06	1	88.38	<0.0001	**
	X_1X_3	0.16	1	4.62	0.0687	
	X_2X_3	0.77	1	22.10	0.0022	**
	X_{12}	0.80	1	23.02	0.0020	**
	X_{22}	2.11	1	60.87	0.0001	**
	X_{32}	14.30	1	412.63	<0.0001	**
	Residual	0.24	7			
	Lack of Fit	0.17	3	3.23	0.1435	
	Pure Error	0.071	4			
	Cor Total	43.64	16			
Y_2	Model	7.15	9	217.82	<0.0001	**
	X_1	2.81	1	769.59	<0.0001	**
	X_2	0.40	1	109.75	<0.0001	**
	X_3	2.61	1	715.38	<0.0001	**
	X_1X_2	4.225E-003	1	1.16	0.3176	
	X_1X_3	0.024	1	6.58	0.0372	*
	X_2X_3	0.014	1	3.95	0.0873	
	X_{12}	1.16	1	317.41	<0.0001	**
	X_{22}	0.036	1	9.77	0.0167	*
	X_{32}	0.040	1	10.86	0.0132	*
	Residual	0.026	7			
	Lack of Fit	0.018	3	3.32	0.1384	
	Pure Error	7.320E-003	4			
	Cor Total	7.18	16			

Note: "$p \le 0.01$" means highly significant (**); "$0.01 < p \le 0.05$" means very significant (*); "$p > 0.05$" means nonsignificant.

$$Y_1 = 1.66 + 1.39X_1 - 0.82X_2 + 0.17X_3 - 0.87X_1X_2 - 0.2X_1X_3 - 0.44X_2X_3 + 0.44X_{12} + 0.71X_{22} + 1.84X_{32} \quad (27)$$

$$Y_2 = 1 + 0.59X_1 + 0.22X_2 - 0.57X_3 - 0.033X_1X_2 + 0.078X_1X_3 - 0.06X_2X_3 + 0.52X_{12} + 0.092X_{22} + 0.097X_{32} \quad (28)$$

As can be seen from the analysis in Table 3, the regression model of seed impurity rate $p<0.0001$, indicating that the regression model is highly significant, and the misfit term p (0.1435) > 0.05, the p value is not significant, indicating that the proportion of non-normal error between the obtained equation and the actual fit is small. The effects of the primary terms X_1 and X_2 of the model are highly significant and X_3 is significant; the interaction terms X_1X_2 and X_2X_3 are highly significant; the secondary terms X_{12}, X_{22}, and X_{32} are highly significant; the remaining items are not significant. According to the magnitude of the regression coefficients of each factor in the regression model, the main order of the influence of each factor on the seed impurity rate can be obtained as X_1, X_2, and X_3, i.e., crank speed, fan speed, and sieve blade opening degree. The coefficient of determination R^2 was 0.9944 and the corrected coefficient of determination R^2_{adj} was 0.9873, both of which are greater than 0.9, indicating that this model can explain the variation of the experiment index effectively.

Similarly, the regression model for scavenging loss rate was

highly significant, with the primary terms X_1, X_2, and X_3 of the model having highly significant effects; The interaction term X_2X_3 had a significant effect; the secondary term X_{12} was highly significant, X_{22} and X_{32} had a significant effect, and the remaining terms were not significant. The main order of influence of each factor on the loss rate is X_1, X_3 and X_2, i.e., crank speed, sieve blade opening degree and fan speed. The coefficient of determination R^2 was 0.9964 and the corrected coefficient of determination R^2_{adj} was 0.9919, both of which were greater than 0.9, indicating that the changes in the experiment indexes could be explained by this model.

4.2.3 Analysis of the interaction effects of experimental factors

Based on the regression model analysis, the corresponding response surface plots were generated using Design-Expert 8.0 software to analyze the effects of the interactions of the experiment factors: crank speed (X_1), fan speed (X_2), and sieve blade opening degree (X_3) on the impurity and loss rates.

(1) Analysis of the effect of seed impurity rate

Figures 11a-11c show the effect of the interaction of factors on the seed impurity rate.

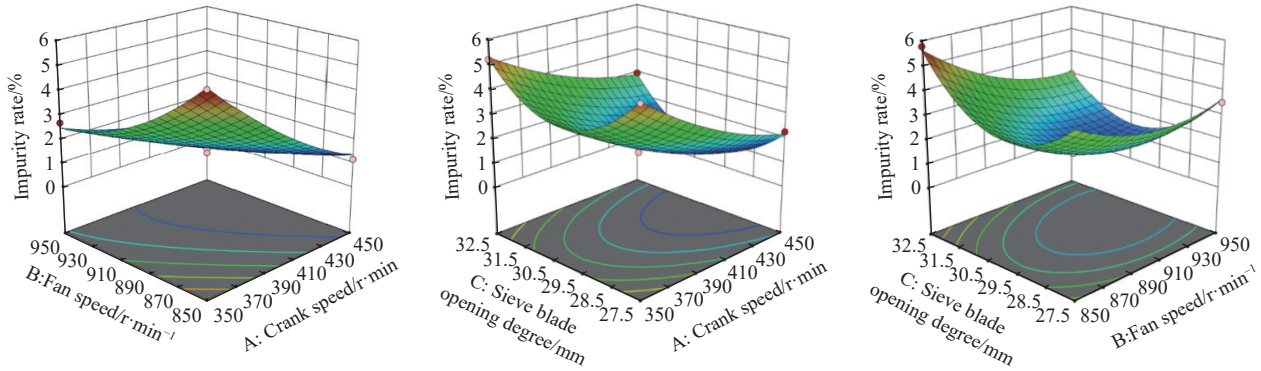

a b c

Figure 11 Effects of factors interaction on seed impurity rate

Figure 11a illustrates the influence of the interplay between crank speed and fan speed on the seed impurity rate when the sieve opening is constant. As the interaction between crank speed and fan speed increases, the rate of impurities in the seeds decreases gradually. This is because the increased crank speed results in an increased vibration frequency of the sieve body, which leads to a shorter contact time between the material components and the sieve surface, and the components are accelerated backward under the action of the forced external force of the sieve body, thus reducing the impurities passing through the sieve. At the same time, the increased fan speed leads to an increased dynamic pressure of the gas at the outlet of the cross-flow fan and an increased airflow speed, which assists in the removal of impurities and thus reduces the rate of impurities.

Figure 11b shows the effect of the interaction of crank speed and sieve blade opening degree on seed impurity rate. As the interaction of crank speed and sieve blade opening degree increases, the seed impurity rate first decreases and then increases. The reason is that when the sieve blade opening degree is 20 mm, the sieve slope is slow, and impurities from the feed inlet fall vertically and collide with the sieve; the center of gravity is on the sieve slope, and the combined force of the air force and the vibration direction of the sieve is greater than the inertia force and friction of the impurities along the sieve downward, and thus the impurities move to the rear of the sieve body, and the rate of impurities is lower than that of seeds. When the sieve opening degree is 30 mm, the sieve slope is steeper, and the center of gravity of the impurities falling and colliding with the sieve is along the sieve downward. The same force of impurities along the sieve slope, combined with the inertial force and friction of the materials in the sieve slope, increases, thus increasing the number of impurities through the sieve and the rate of impurities.

Figure 11c shows the effect of the interaction of fan speed and sieve opening on the seed impurity rate. When the interaction between fan speed and sieve blade opening degree increased, the impurity rate first decreased and then increased, but the increase is slightly greater than that of Figure 11b. This is because the adjustment of the sieve adjustment mechanism changes the slope angle of the sieve, resulting in a change in the direction and size of the airflow through the upper and lower surfaces of the sieve. As the sieve opening degree gradually increases from 20 mm, the slope of the sieve gradually steepens, the air flow on the upper and lower surfaces of the sieve in the direction of airflow from the fan outlet increases, and the number of impurities moving to the rear of the sieve body increases, leading to a decrease in the impurity rate. With a further increase in the sieve opening degree, the air flow on the upper and lower surfaces of the sieve decreases, leading to increased numbers of impurities passing through the sieve and a consequent increase in the impurity rate.

(2) Analysis of the effect of the cleaning loss rate

Figures 12a-12c show the effects of the interaction of factors on the loss rate of cleaning.

As shown in Figure 12a, the cleaning loss rate gradually increases with the increase in the interaction between crank speed and fan speed. The reason is that the increase in crank speed leads to an increase in the vibration frequency of the sieve body, while the increase in fan speed results in an increase in airflow speed, thus making seeds with smaller grain sizes blow out of the machine and increasing the loss rate.

As shown in Figure 12b, the interaction between crank speed and sieve opening degree increases, the cleaning loss rate gradually increases. With the increase in crank speed, the cleaning loss rate increases continuously. When the sieve opening degree increases, the material penetration speed is lower than the material throwing speed to the back of the sieve, resulting in an increase in the loss rate in general.

As shown in Figure 12c, the cleaning loss rate slightly decreases with the increasing interaction between fan speed and sieve opening. With the increase in fan speed, the dynamic pressure at the air outlet increases, causing some small seeds to be blown out of the machine. Meanwhile, the sieve opening gradually increases, which mitigates the loss of seeds. However, the effect of fan speed on the loss rate is slightly more significant than that of sieve opening, resulting in an overall increased loss rate.

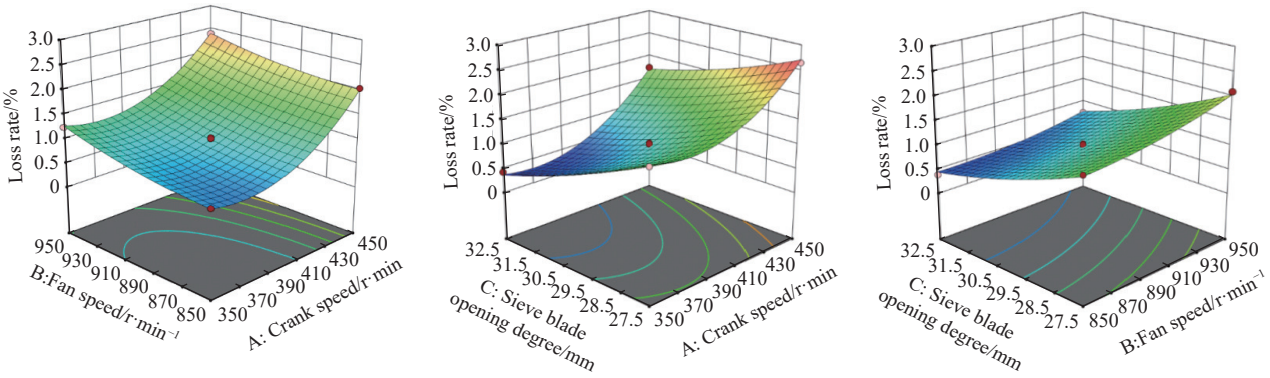

Figure 12 Effect of interaction of factors on cleaning loss rate

4.2.4 Parameter optimization

In order to achieve the optimal performance of the wind sieve type *Cyperus esculentus* cleaning device, the minimum values of impurity rate and loss rate are required, and the minimum values of seed impurity rate and cleaning loss rate are taken as the optimization indices. A full factorial quadratic regression equation of the performance indices is established to optimize the objective and determine the optimal working parameters.

$$\min E(X) = \begin{cases} Y_1(X_1, X_2, X_3) \\ Y_1(X_1, X_2, X_3) \end{cases} \quad (29)$$

Among them

$$\begin{cases} 400 \le X_1 \le 500 \\ 800 \le X_2 \le 900 \\ 20 \le X_3 \le 30 \end{cases} \quad (30)$$

Using the Optimization function provided by the Design-Expert software and setting the above factors as the constraints, with the regression model equation of impurity rate and loss rate as the objective function, the minimum value was obtained and the optimum factor parameters were identified: crankshaft speed 445.13 r/min, fan speed 865.88 r/min, and sieve opening 26.61 mm. After rounding the optimal parameter combination to 445 r/min, 866 r/min, and 27 mm, respectively, the predicted impurity rate and loss rate under this condition were 1.78% and 0.84%, respectively.

4.3 Experimental validation

In order to verify the reliability of the regression model, a wind sieve-type oleaginous bean cleaning device was employed for performance experiments, as shown in Figure 13. Five operational performance experiments were conducted according to the predicted values of the above optimal parameter combinations, with the shaker inverter set to 21.2 Hz and the fan inverter set to 43.3 Hz, using the same experiment materials and methods as described in Sections 2.1 and 2.2. Under five experiments, the average impurity rate and average cleaning loss rate of seeds were 1.88% and 0.87%, respectively, and the relative errors of the experiment values and the predicted values were 5.69% and 3.57%, respectively. The results showed that the wind sieve-type *Cyperus esculentus* cleaning device could effectively reduce the impurity rate and cleaning loss rate of seeds under the optimized working parameters. Moreover, the established regression model was reliable, and the working and structural parameters of the wind sieve-type *Cyperus esculentus* cleaning device were reasonably designed.

To verify the application of the stand on the whole machine, according to "GB/T 8097-2008 Harvesting Machinery Combine Harvester Experiment Method", the total length of the experiment area was set to 40 m, and the middle 20 m was taken as the stable measurement area. The same working condition was repeated three times, and the mixture collected in the bin was taken to measure the seed impurity rate; the ratio of the seeds dropped on the ground behind the whole machine and the excavated whole *Cyperus esculentus* was taken as the cleaning loss rate, and the results were averaged. The average values of seed impurity rate and cleaning loss rate were 3.54% and 1.23%, respectively, which met the harvesting requirements of the combine harvester, as shown in Figure 14. The field verification is shown in Figure 15.

Figure 13 Operation validation of the wind sieve type cleaning device

a. Cyperus esculentus collected in general b. Cyperus esculentus

Figure 14 Comparison of the collected *Cyperus esculentus* collected after parameter optimization

Figure 15 Verification of field operation of *Cyperus esculentus* combine harvester

5 Limitations and prospects

5.1 Limitations

(1) This study focuses on the effectiveness of *Cyperus esculentus* cleaning in a sandy soil environment. It is not applicable to the harvesting of *Cyperus esculentus* grown in other soil types.

(2) Although the single-factor experiments and response surface methodology employed in this study prove effective, they fail to account for all potential interactions and influencing factors, such as ambient temperature and mechanical wear during the cleaning process.

(3) The equipment developed in this study is designed specifically for *Cyperus esculentus* and may not deliver optimal results when cleaning similar crops.

5.2 Prospects

(1) Future research could further optimize and improve the equipment and conduct field trials under diverse soil conditions, such as different humidity levels and different types of soil environments, to improve applicability and effectiveness under a wider range of conditions.

(2) Researchers are advised to adopt more comprehensive experimental designs, such as factorial design or multilevel analysis, to explore the interactions between various variables and their combined impact on cleaning efficiency.

(3) Future studies should explore adjusting equipment parameters or designs to accommodate a wider range of crops, which will expand the equipment's applications and enhance its versatility and flexibility during the crop cleaning process.

6 Conclusions

(1) In this study the efficacy of an "airflow + vibration" dual-action cleaning method was established based on the analysis of the suspension speeds of different components in the threshing mixture. A closed vector model was employed to elucidate the dynamics of the vibrating sieve, including acceleration, velocity, and trajectory in a simple harmonic motion with a fixed amplitude. A novel approach was also presented to constructing a force model for seed interaction with the sieve surface, facilitating an understanding of the conditions necessary for seed movement along the sieve. Additionally, a geometric model was developed for the adjustable sieve blade mechanism, enabling precise control over the sieve blade rotation. The optimal structural parameters of the sieve surface were determined that allow seed penetration while preventing stalk passage, and the re-throwing process of long stalks was analyzed to define the key parameter ranges critical for efficient separation.

(2) Through single-factor experiments, the variation patterns of seed impurity and cleaning loss rates under different operational parameters were analyzed. A comprehensive three-factor, three-level response surface analysis was conducted by Box-Behnken design. And a second-order regression model was developed that provides insight into the significant impact of each factor and their interactions on the evaluation indices. The findings reveal that the most influential factors on seed impurity rate are crank speed, fan speed, and sieve blade opening degree in a descending order. In contrast, for the cleaning loss rate, the order of significance is crank speed, sieve blade opening degree, and fan speed. The optimal operational parameters were determined as crank speed of 445 r/min, fan speed of 866 r/min, and a sieve opening of 27 mm, achieving minimum seed impurity (1.78%) and cleaning loss rates (0.84%). The validation of these parameters in field experiments confirmed an average seed impurity rate of 1.88% and a cleaning loss rate of 0.87%, indicating the high accuracy of our regression model and its practical applicability in meeting harvesting requirements.

Acknowledgements

This is work was financially supported by the Division City Science and Technology Achievement Transformation Guidance Plan Project (Development and demonstration of *Cyperus esculentus* harvesting machine in sandy areas of Xinjiang) (Grant No. KJ2023CG01); the Science and Technology Plan Project of the Corps - Science and Technology Talent Category: Analysis of Clogging Process of Roller Screen Holes in Cyperus esculentus Harvester and Research on Reverse Friction Declogging Methods (Grant No. 2024DB016), and the Science and Technology Research Program of Shihezi University: Development and Demonstration of High-Efficiency Harvesting Equipment for Cyperus esculentus Using Dual-Layer Differential Speed Roller Screens (Grant No. KJGG202404).

[References]

[1] Wu J J, Lang C X, Wang F L, Liu R H, Zheng T, Wu G T. Production and development status of edible vegetable oils and improvement progresses of their fatty acid compositions in China. China Oils and Fats. 2020; 45(5): 4–10. (in Chinese)

[2] Guo T T, Wan C Y, Huang F H, Wei C L, Hu Z H. Research progress on the main nutritional components and physiological functions of tiger nut (*Cyperus esculentus* L.). Chinese Journal of Oil Crop Sciences, 2021; 43(6): 1174–1180. (in Chinese)

[3] Qi J T, An S G, Kan Z, Meng H W, Li Y P, Zhao X Y. Discrete element-based calibration of simulation parameters of *Cyperus esculentus* L. (tiger nut) planted in sandy soil. J Food Process Pres, 2021; 45(7): e15631.

[4] Zhang X T, Wu X Q. Cultivation and production potential evaluation of *Cyperus esculentus* L. in marginal land of Inner Mongolia. Transactions of the CSAE, 2022; 38(2): 289–295. (in Chinese)

[5] Liu Y L, Zhao Y, Xu M Q, Chai X T, Zeng F J, Li X Y, Li L, Huang C B. Effect of row spacing on the growth of *cyperus esculentus* and soil properties in extremely arid region. Acta Agrestia Sinica, 2021; 29(11): 2486–2493.

[6] Wang R Y, Wang X S, Xiang H. A multi-purpose novel oil crop—Cyperus beans. China Oils and Fats, 2019; 44(1): 1–4.

[7] Wang X, Li Z. Tigernut industry in China: current status of development, potential and adaptive suggestions. Chinese Journal of Oil Crop Sciences, 2022; 44(4): 712–717. (in Chinese)

[8] Sánchez-Zapata E, Fernández-López J, Pérez-Alvarez J A. Tiger nut (*Cyperus esculentus*) commercialization: Health aspects, composition, properties, and food applications. Compr Rev Food Sci F, 2012; 11(04): 366–377.

[9] Sa´nchez-Zapata E, Fuentes-Zaragoza E, Ferna´ndez-lo´pez J, Sendra E, Sayas E, Navarro C, Pérez-Alvarez J A. Preparation of dietary fiber powder from tiger nut (*Cyperus esculentus*) milk ("Horchata") byproducts and its physicochemical properties. J. Agric. Food Chem., 2009; 57: 7719–7725.

[10] Xu L Z, Li Y, Li Y M, Chai X Y, Qiu J. Research progress on cleaning technology and device of grain combine harvester. Transactions of the CSAM, 2019; 50(10): 1–16. (in Chinese)

[11] Liu P, Jin C Q, Yang T X, Chen M, Ni Y L, Yin X. Design and experiment of multi parameter adjustable and measurable cleaning system. Transactions of the CSAM, 2020; 51(S2): 191–201. (in Chinese)

[12] Wang L, Li Y, Liang C, Ma J Q, Zhou W X. Motion law of maize mixture in cross air-and-screen cleaning device. Transactions of the CSAM, 2015; 46(9): 122–127. (in Chinese)

[13] Hu Z C, Wang B, Yu Z Y, P B L, Zhang Y H, Tan L K. Design and test of semi-feeding test-bed for peanut pod picking. Transactions of the CSAE, 2017; 33(17): 42–50. (in Chinese)

[14] Zhang M, Jin C, Liang S, Tang Q, Wu C Y. Parameter optimization and experiment on air-screen cleaning device of rapeseed combine harvester. Transactions of the CSAE, 2015; 31(24): 8–15. (in Chinese)

[15] Dai F, Fu Q F, Zhao W Y, Shi R J, Song X F, Zhang S L. Design and Test of Double Duct System of Air-screen Separating and Cleaning Machine for Flax Threshing Material. Transactions of the CSAM, 2021; 52(4): 117–125, 247. (in Chinese)

[16] Yang Meng, Zhang Y H, Zhang C, Gu F W, Yu Z Y, Hu Z C. Design and experiment of fan-sieve combined peanut film- seedling separating device based on shredding and separating. Transactions of the CSAM, 2020; 51(12): 112–121. (in Chinese)

[17] Wang L J, Ma Y, Feng X, Song L L, Chai J. Design and experiment of segmented vibrating screen in cleaning device of maize grain harvester. Transactions of the CSAM, 2020; 51(9): 89–100. (in Chinese)

[18] Li Y, Xu L Z, Zhou Y, Li B J, Liang Z W, Li Y M. Effects of throughput and operating parameters on cleaning performance in air-and-screen cleaning unit: A computational and experimental study. Comput. Electron. Agr, 2018; 152: 141–148.

[19] Xu L Z, Li Y, Chai X Y, Wang G M, Liang Z W, Li Y M, Li B J. Numerical simulation of gas-solid two-phase flow to predict the cleaning performance of rice combine harvesters. Biosyst. Eng, 2020; 190: 11–24.

[20] Geng D Y, Mu X D, Zhang G, Wang Z Y, Zhu J K, Xu H G. Analysis and optimization of cleaning mechanism of wheat combine harvester. Journal of Jilin University (Engineering and Technology Edition), 2022; 52(1): 219–230.

[21] Liu X M, Liu Z H, Liang Y, Xiao S P. Development of multifunctional harvesting machine based on modular theory. Journal of Chinese Agricultural Mechanization, 2012; 243(5): 47–50.

[22] Qu Z, Han M H, Lv Y L, Zhou Z, Lv Z J, Wang W Z, He X. Design and test of a crawler-type tiger-nut combine harvester. Agriculture, 2023; 13(2): 277.

[23] He X, Lv Y L, Qu Z, Wang W Z, Zhou Z, He X. Parameters optimization and test of caterpillar self-propelled tiger nut harvester hoisting device. Agriculture, 2022; 12(7): 1060.

[24] Shu C X, Yang J, Wan X Y, Yuan J C, Liao Y T, Liao Q X. Calibration and experiment of the discrete element simulation parameters of rape threshing mixture in combine harvester. Transactions of the CSAE, 2022; 38(9): 34–43. (in Chinese)

[25] Zhu C H, Chen B, Li J Q, Liu Y, Yang L Q, Wang W Z, Zhang H M. Design and testing of the peanut pod cleaning device. Agriculture, 2023; 11(1): 106.

[26] Tang H, Xu C S, Wang Z M, Wang Q, Wang J W. Optimized design, monitoring system development and experiment for a long-belt finger-clip precision corn seed metering device. Front. Plant Sci, 2022; 13: 814747.

[27] Li L, Zhang S, He Q, Hu X B. Application of response surface methodology in experiment design and optimization. Research and Exploration in Laboratory, 2015; 34(8): 41–45.

[28] Takagi D, Shimada T. A Spatial regression analysis on the effect of neighborhood-level trust on cooperative behaviors: Comparison with a multilevel regression analysis. Front. Psychol, 2019; 10: 2799.